

Preliminary Electromagnetic and Mechanical Design of a $\cos\theta$ Dipole for the Muon Collider Study

Francesco Mariani, Luca Alfonso, Andrea Bersani, Luca Bottura, Barbara Caiffi, Stefania Farinon, Samuele Mariotto, Daniel Novelli, Alessandra Pampaloni, Tiina Salmi, Stefano Sorti, Lucio Rossi, *Fellow, IEEE*

Abstract—Within the framework of the International Muon Collider Collaboration (IMCC), an innovative feasibility study on a Muon Collider accelerator complex is currently under development, granted by the European Union through Agreement 101094300. The proposed goal aims to develop a 10 km collider ring accelerating muons at approximately 10 TeV in the center-of-mass frame. To achieve this target, several requirements on the collider design arise to maximize the luminosity despite the short lifetime of this type of particle at rest. Despite being operated in steady-state mode, the superconducting magnet dipoles of the main collider are presently evaluated as the most challenging technological development of the design study. High levels of magnetic field above 10 T are presently foreseen with a magnet bore diameter around 150 mm to accommodate a tungsten shielding for the muon decay heat deposition. To minimize the radiation dose, coming from the collimated neutrino beams, different types of combined dipole and quadrupole are also considered in the lattice reducing the straight sections in the collider at the expense of the magnet performances and feasibility. An analytical analysis of possible magnet performances with the available technology has been already developed suggesting different working points for the magnet design. In this contribution, a first proposal of 2D $\cos\theta$ electromagnetic and mechanical designs is provided comparing the analytical approach with FEM (Finite Element Method) - optimized configurations. HTS (High Temperature Superconductor) superconducting magnet designs have been evaluated to estimate the maximum possible expected performances of the collider, minimize the magnet cost, and deal with the requirements for the cryogenic cooling of the entire accelerator complex.

Index Terms—High Field Superconducting Magnets, Screening Current, Magnetization in REBCO tape.

I. INTRODUCTION

THE IMCC [1] is presently developing a feasibility study for the realization of a 10 TeV, 10 km Muon Collider accelerator complex providing the same physics discovery

F. Mariani is with Sapienza University of Rome, 00185 Rome, Italy, and also with Laboratory of Acceleration and Applied Superconductivity, INFN-Milano, 20054 Milan, Italy. (email: francesco.mariani@mi.infn.it)

S. Mariotto, L. Rossi, S. Sorti are with the Department of Physics, University of Milan, 20133 Milan, Italy and Laboratory of Acceleration and Applied Superconductivity, INFN-Milano, 20054 Milan, Italy.

L. Alfonso, A. Bersani, B. Caiffi, A. Pampaloni are with the National Institute for Nuclear Physics (INFN-Genova), 16146 Genoa, Italy.

D. Novelli is with Sapienza University of Rome, 00185 Rome, Italy, and also with INFN-Genova, 16146 Genoa, Italy.

T. Salmi is with Tampere University, 33720 Tampere, Finland.

L. Bottura is with the European Organization for Nuclear Research (CERN), 1211 Geneva, Switzerland.

On behalf of IMCC.

Manuscript received August 00, 2023; revised August 00, 2023.

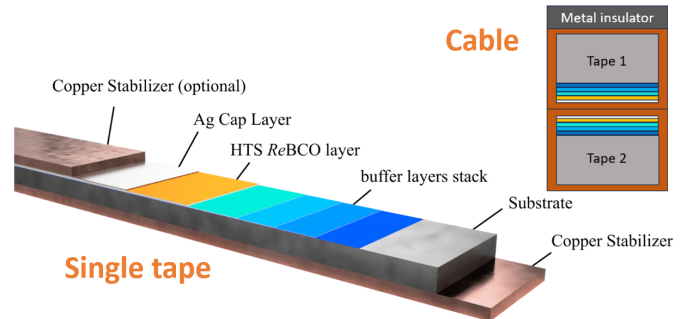


Fig. 1. On the left, tape composition rendering (courtesy of S. Mariotto). On the right, “two-in-hand” cable.

potential of hadron-based colliders, working at higher energies in the center-of-mass frame, with lower realization cost and energy consumption [2]. The collider ring presently features high field steady state superconducting magnets in the range 16–20 T, providing high luminosity and compact dimension of the tunnel, with large bore aperture diameters up to 140 mm to shield the superconducting coil from the decay products of the muon beam [3], [4]. An analytical approach, supported by numerical analysis, allowed for the definition of the performance limits for superconducting dipoles and quadrupoles, depending on the superconducting technology and magnet operating condition and limitations, and rapidly iterated on the superconducting magnet design for the beam lattice optimization [5], [6]. Thanks to this method, a 16 T dipole magnet with a bore aperture of 140 mm, entirely made in HTS technology and operating at 20 K [7] was considered in a $\cos\theta$ design [8], as a case study of the preliminary electromagnetic and mechanical optimization of the magnet cross-section.

II. MAGNET DESIGN

Since the high field and the high operational temperature require the use of HTS technology, similarly to ESMA magnet [9], [10] and in agreement with the accelerator magnet [11] and the collider magnet in block coil configuration [12], a cable made by two Fujikura REBCO tapes (FESC-SCH12) [13] co-wound with a stainless-steel tape has been considered for the superconducting coil layout. The tape is 12 mm wide and 110 μm thick. Within its 20 μm thick copper coating, it includes several materials: a Hastelloy layer for mechanical

TABLE I
PRINCIPAL PROPERTIES OF THE MAGNET.

Parameters and Results	Value
Central field	16 T
Peak field	17.6 T
Current	1702 A
Engineering current density (inner)	525 A/mm ²
Engineering current density (outer)	579 A/mm ²
Operating temperature	20 K
Temperature margin	8 K
Inductance	3.4 H/m
Stored energy	4.9 MJ/m
Total tape length	10.736 km/m

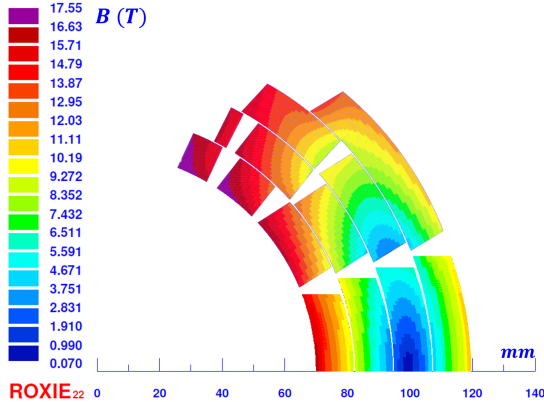


Fig. 2. Magnet layout and field map with uniform current density.

stability, buffer layers for superconductor deposition, the superconductive layer of thickness $2.5 \mu\text{m}$, and a protective silver layer $2 \mu\text{m}$ thick that prevents the copper from reacting with the superconductor (see Fig. 1). Between cables, a stainless steel metal-insulator (dark gray in Fig. 1) was introduced to enhance the quench protection. Its thickness is $50 \mu\text{m}$ for inner layers and $25 \mu\text{m}$ for outer layers. In Table I the main parameters of the magnet, considering a uniform current density, are listed. The coils layout is shown in Fig. 2 [14], exhibiting 4 layers with 4, 4, 3, and 2 blocks respectively, for a total of 1342 turns. The advantages of using HTS instead of LTS (Low Temperature Superconductor) technology are several:

- the higher B_{c2} allows to generate higher field without quenching;
- the higher current density means a more compact magnet;
- the higher T_c makes it possible to operate at higher temperatures, thus reducing the refrigeration cost.

However, due to their material properties, quench protection of HTS coils is more challenging [15], and cables of REBCO tapes are in general more expensive than LTS cables. In addition, the wide width of tapes and their non-transposed configuration inside the cables generate high magnetization leading to high hysteretic losses and non-uniform field quality. This magnetization is produced by the screening current taking place inside each superconductive layer to cancel the perpendicular field inside (due to the small thickness of the superconductive layer, we can neglect the current distribution along the thickness of the tape induced by the parallel

component of the field). The scope of the study reported in this paper is the analysis of the current distribution inside the tapes of a geometrically optimized coil cross-section and their effect on the electromagnetic and mechanical design of the magnet. Below, the paper is subdivided into three sections: the first one briefly introduces the Brandt model [16] used to describe the current distribution inside a single REBCO tape immersed in a uniform perpendicular field. At the end of this paragraph, the limit of this model is discussed and its influence on the obtained results is described. In the second section, electromagnetic study results are shown. The last section is dedicated to a preliminary mechanical analysis performed with COMSOL [17] to evaluate the stresses produced by the non-uniform current distribution. Then, some possible solutions to guarantee mechanical stability are discussed.

III. CURRENT DISTRIBUTION IN A $\cos\theta$ DIPOLE MAGNET MADE WITH REBCO TAPES

To calculate the non-uniform current distribution of the 16 T $\cos\theta$ dipole magnet, a MATLAB code has been used to implement the Brandt model inside the tape cross-section. This model, developed by E. H. Brandt and M. Indenbom in 1993, describes how the *sheet current* J (A/mm) (i.e. the current density integrated along the thickness of the tape - see details in [16]) distributes inside a single REBCO tape immersed in a uniform perpendicular field B_{\perp} . Three main aspects are considered:

- 1) when the tape is immersed in a magnetic field, a screening current J_{screen} is induced to cancel the inner perpendicular field. Flux starts to penetrate at the edges and, considering a type II superconductor, J_{screen} is limited to the critical value near the edges $J_{screen} = j_c d$ where j_c (A/mm²) is the critical current density and d is the tape thickness (see Fig. 3.a);
- 2) as the field increases, J_{screen} (that cannot overcome the critical value) penetrates towards the center of the tape, thus reducing the zero field region (see Fig. 3.b);
- 3) if a transport current J_t flows along the tape, two different scenarios need to be distinguished:
 - A. if J_{screen} has not yet fully penetrated inside the tape (see Fig. 3.c), then J_t will distribute in the region not yet saturated (see Fig. 3.d);
 - B. if J_{screen} has fully penetrated (see Fig. 3.e), then J_t will distribute in the central region of the tape by pushing J_{screen} towards the edges reducing its intensity (see Fig. 3.f).

One of the main differences between the Brandt model and the Bean model is the following: when the flux has partially penetrated and the critical state $J = J_c$ is established near the edges of the specimen, the current flows over the entire width of the tape to shield the central flux-free region (in the Bean model, the flux-free region is current free) (see [16], pag.1-2).

To calculate how the current distributes inside this region, Brandt and Indenbom started by considering that a uniform current flowing along a cylinder of circular cross-section does not generate a field inside the cylinder. So, by conformal mapping, the current distribution inside a tape of rectangular

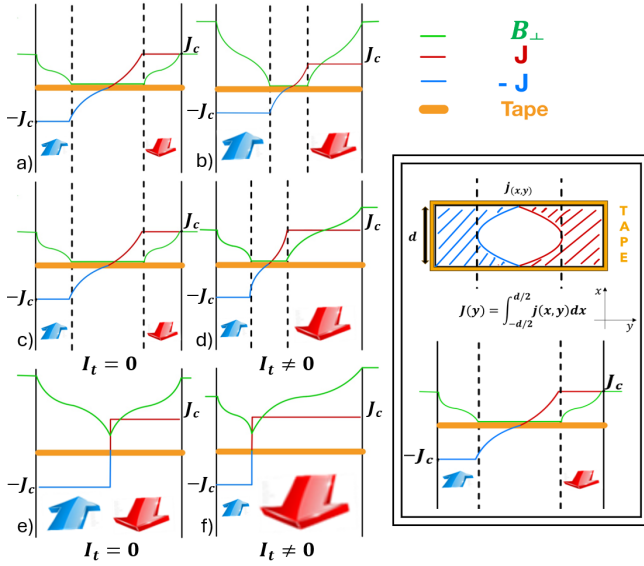


Fig. 3. a) no I_t , low field. b) no I_t , high field. c) no $I_t = 0$, no saturation. d) $I_t \neq 0$, no saturation. e) $I_t = 0$, saturation f) $I_t \neq 0$, saturation. On the right, description of *sheet current* J as the current density $j(x, y)$ integrated along the thickness d .

cross-section can be obtained to create the same effect. After having analyzed separately how the external field and the transport current affect the current distribution along the tape width, the sheet current distribution, considering both induced current density and transport current, can be described as

$$J = Jc[j(y + w, a + w, b) + pj(-y - w, -a - w, b)] \quad (1)$$

where j (that is adimensional and must not be confused with the current density) is the following step function

$$j(y, a, b) = \begin{cases} 1, & \text{if } b \leq y \leq a \\ \frac{1}{\pi} \operatorname{arccot} \frac{b^2 - ay}{p}, & \text{if } -b \leq y \leq b \\ 0, & \text{if } -\infty < y \leq -b \end{cases}$$

In Eq. 1, a represents the half-width of the tape, $p = +1$ if the effect of the transport current on the current distribution is greater than the effect of the external field, and $p = -1$ otherwise. The variables b and w are

$$b = \frac{b_1 + b_2}{2} \geq 0, \quad w = \frac{b_1 - b_2}{2} \geq 0$$

where $a - b_1$ and $a - b_2$ are respectively the penetration depths along the left and right sides of the tape. The values for b and w depend on transport current and external field, see [16].

A. Limit and Mitigation of Brandt Model.

The model's previously described limit consists in the assumption of a uniform perpendicular field around the tape. Hence, to evaluate how the current distributes inside the coils of the $\cos\theta$ magnet, the mean value of the perpendicular field along each tape was calculated and then assumed as the uniform perpendicular field value around that tape. Since the magnet is made by multiple turns, to calculate the current distribution for each value of transport current and position in the magnet cross-section, appropriate convergence algorithms have been used considering the mutual interaction of tapes.

IV. ELECTROMAGNETIC ANALYSIS

The electromagnetic results obtained by the code are now presented. In Fig. 4 the current distribution during energization is shown. It is evident that the current penetration depth is strongly influenced by the orientation of the tapes and their position within the cross-section. Indeed, since the magnetic field is approximately parallel to the tapes of the third layer, these tapes are far from saturation (J_{screen} flows only near the edges). Since the screening current attenuates the perpen-

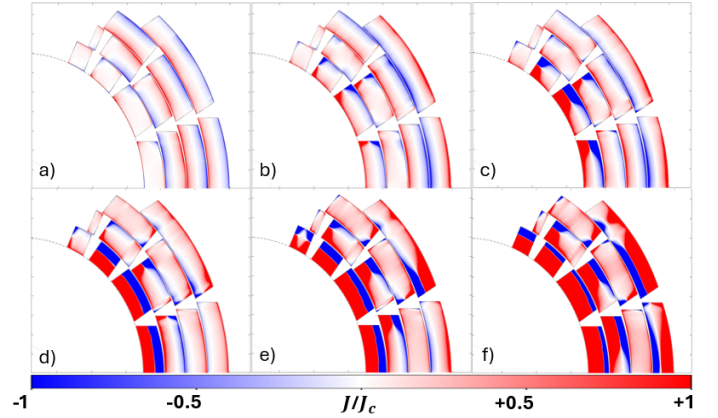


Fig. 4. Red positive current outgoing, blue negative current. a) $I_t = 250$ A b) $I_t = 500$ A c) $I_t = 750$ A d) $I_t = 1000$ A e) $I_t = 1350$ A f) $I_t = 1702$ A

dicular field (the most effective field component in reducing the critical current of the tape), the margin to quench of each block increases (see Fig. 5).

Multipoles	J_{unif}	$J_{non\ unif}$
b_3	0.05	6.6
b_5	1.2	0.7

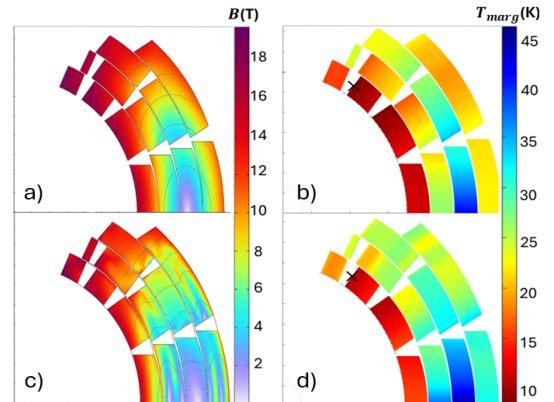


Fig. 5. a) Field map at nominal current without screening current, i.e. J_{unif} and c) with screening current, i.e. $J_{non\ unif}$. b) Temperature margin map at nominal current without screening current and d) with screening current (the 'x' symbol indicates the location of the minimum margin).

Figure 5 also shows the field quality comparison between uniform (no screening current) and non-uniform current distribution (i.e. with screening current). The non-uniform current distribution increases sextupole error, thus reducing the field quality. In Fig. 6 hysteretic losses per meter length during energization are presented. Calculation of losses was performed

by considering for each tape the magnetization produced by the current distribution flowing inside it.

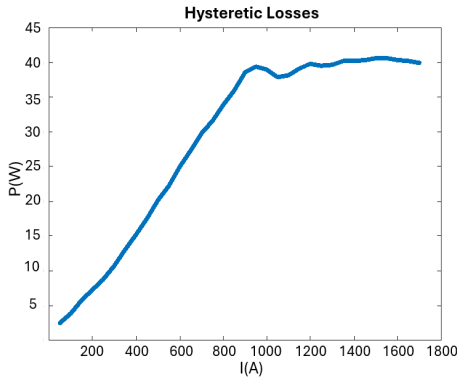


Fig. 6. Losses per meter during first energization.

Assuming a time of charge of 20 minutes, the hysteretic losses produced by each tape were obtained by the following formula:

$$P = M \cdot \frac{dB}{dt} \quad (2)$$

where $M(A/m)$ is the magnetization. As the figure shows, power losses initially grow as the screening current effect increases. The peak value of 40 W/m is reached around a transport current intensity of 1500 A. From 1000 A to nominal current, hysteretic losses reach a plateau. Indeed, during the increase of hysteretic currents in the outer layer, the transport current suppresses the magnetization current in the inner layers reducing their hysteretic losses contribution. As result, the overall contribution of screening currents to the losses remains almost unchanged. Since even a ramp time of 200 minutes might be acceptable for MuCol, hysteretic losses would be reduced by a factor of 10 (for the same amount of energy dissipated), making them much more manageable.

V. MECHANICAL ANALYSIS

The screening current affects somehow also the mechanical design. To evaluate its impact, the current distribution obtained by MATLAB code was imported in COMSOL, where a mechanical study was performed comparing two model assumptions:

- the former assumes the four layers to be bonded together (an assumption especially made when LTS technology is used, since coils are usually impregnated and consequently all the layers are not free to move or detach from each other);
- the latter considers separation and frictionless contact between winding layers.

Both models have in common the following assumptions:

- the collar around the magnet was modeled and supposed to be infinitely rigid;
- the contact between collar and layers was considered to be frictionless;
- the Young modulus for coil layers of 174 GPa [18] has been calculated using a homogeneous material where average properties of the cable have been considered.

With this assumption, empty spaces between cables and layers are not taken into account;

- wedges are supposed to be made of copper.

Figure 7 shows for both models the azimuthal stress produced by the Lorentz forces generated by the non-uniform current distribution. The tensile stress at the top of the magnet should

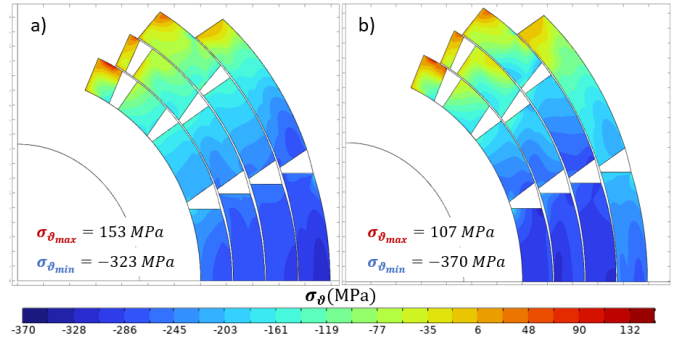


Fig. 7. Comparison between azimuthal stress produced in case of a) bonded layers and b) separated layers in frictionless contact.

be canceled to avoid delamination of the tapes. The maximum compressive stress for both models is below the threshold of 400 MPa [19]. The configuration with separated layers (Fig. 7.b) could be effective in reducing the tensile stress, even if the compressive stress slightly increases. Furthermore, the maximum midplane stress in this case doesn't take place in the outer layer but in the third one. Taking into account these differences, only a more in-depth study will allow to assess the real performance of the mechanical design of the magnet.

VI. CONCLUSIONS

To design a $\cos\theta$ dipole magnet, using only HTS conductors, the non-uniform current density distribution has to be taken into account due to the non-negligible magnetization coming from the wide width of REBCO tapes and their non-transposed disposition inside the cable. Relying on the Brandt model, it was possible to obtain a first estimation of the losses taking place during the ramping time and how field quality is affected by magnetization. A preliminary design has been developed satisfying the following requirements: central field $B = 16$ T, bore aperture $d_{bore} = 140$ mm, operational temperature $T_{op} = 20$ K, temperature margin $\Delta T = 2.5$ K. The tensile stress at the top of the magnet must be canceled, whereas the compressive stress on the midplane is below the threshold value. Hysteretic losses are acceptable considering a ramping time of about 200 minutes. A more detailed mechanical and thermal analysis, together with a quench study, will be performed to ensure adequate stability and protection to the magnet. However, the study presented here was essential to evaluate the influence of magnetization currents on field quality, forces and losses. Further improvements of the code for current distribution evaluation will be performed to obtain more accurate results.

ACKNOWLEDGEMENT

The authors thank the PNRR-IRIS project of INFN funded by the Italian Ministry of Research for the financial support.

REFERENCES

- [1] C. Accettura *et al.*, “Towards a muon collider,” *The European Physical Journal C*, vol. 83, no. 9, pp. 1–110, 2023.
- [2] C. Adolphsen *et al.*, “European Strategy for Particle Physics–Accelerator R&D Roadmap,” *arXiv preprint arXiv:2201.07895*, 2022.
- [3] L. Bottura *et al.*, “A work proposal for a collaborative study of magnet technology for a future muon collider,” *arXiv preprint arXiv:2203.13998*, 2022.
- [4] L. Bottura *et al.*, “Magnets for a Muon Collider—Needs and Plans,” *IEEE Transactions on Applied Superconductivity*, vol. 34, no. 5, pp. 1–8, 2024.
- [5] D. Novelli *et al.*, “Analytical and numerical study of superconducting dipole and quadrupole performance limits for a Muon Collider,” *IEEE Transactions on Applied Superconductivity*, 2024.
- [6] D. Novelli *et al.*, “Analytical Evaluation of Dipole Performance Limits for a Muon Collider,” Submitted to IEEE TASC to be published, 2024.
- [7] P. B. de Sousa *et al.*, “Muon collider magnet technology options internal review-cooling,” in *IMCC Annual Meeting*, 2023, pp. 19–22.
- [8] B. Caiffi *et al.*, “Challenges and Perspectives of the Muon Collider Ring Superconducting Magnets,” Submitted to IEEE TASC to be published, 2024.
- [9] S. Maffezzoli Felis *et al.*, “An update on IRIS demonstrators,” no. 15, pp. 2909–2911, 05 2024. [Online]. Available: <https://indico.jacow.org/event/63/contributions/4161>
- [10] L. Rossi *et al.*, “Design and plan of a 10 T HTS energy saving dipole magnet for the Italian facility IRIS,” *IEEE Transactions on Applied Superconductivity*, 2024.
- [11] F. Levi *et al.*, “Magnetic and mechanical design of the large aperture hts superconducting dipoles for the accelerator ring of the Muon Collider,” Submitted to IEEE TASC to be published, 2024.
- [12] L. Alfonso *et al.*, “Preliminary Design of a Block-Coil Magnet for the Muon Collider Ring,” *IEEE Transactions on Applied Superconductivity*, pp. 1–5, 2024.
- [13] Fujikura hts tape online catalogue. [Online]. Available: <https://www.fujikura.co.uk/netalogue/pdfs/Fujikura%20Superconductor%20Guide.pdf>
- [14] S. Russenschuck, “<https://espace.cern.ch/roxie>.”
- [15] T. Salmi *et al.*, “Estimation of quench protection limits in REBCO dipoles and quadrupoles,” Submitted to IEEE TASC to be published, 2024.
- [16] E. H. Brandt and M. Indenbom, “Type-II-superconductor strip with current in a perpendicular magnetic field,” *Physical review B*, vol. 48, no. 17, p. 12893, 1993.
- [17] C. Multiphysics, “<https://www.comsol.com>.”
- [18] C. Barth *et al.*, “Electro-mechanical properties of REBCO coated conductors from various industrial manufacturers at 77 K, self-field and 4.2 K, 19 T,” *Superconductor Science and Technology*, vol. 28, no. 4, p. 045011, 2015.
- [19] [Online]. Available: <https://www.fujikura.co.jp/eng/products/newbusiness/superconductors/01/superconductor.pdf>